ACS APPLIED MATERIALS & INTERFACES

Research Article

www.acsami.org

Chemically Tunable Ultrathin Silsesquiazane Interlayer for n-Type and p-Type Organic Transistors on Flexible Plastic

Wi Hyoung Lee,[†,▽] Seung Goo Lee,[‡,▽] Young-Je Kwark,[§] Dong Ryeol Lee,[∥] Shichoon Lee,[⊥] and Jeong Ho Cho*[,#]

[†]Department of Organic and Nano System Engineering, Konkuk University, Seoul 143-701, Korea

[‡]Department of Chemical Engineering, Massachusetts Institute of Technology, Cambridge, Massachusetts 02139, United States

[§]Department of Organic Materials and Fiber Engineering, Soongsil University, Seoul 156-743, Korea

[∥]Department of Physics, Soongsil University, Seoul 156-743, Korea

[⊥]Department of Materials Science and Engineering, Jungwon University, Goesan 367-805, Korea

[#]SKKU Advanced Institute of Nanotechnology (SAINT) and School of Chemical Engineering, Sungkyunkwan University, Suwon 440-746, Korea

ABSTRACT: In organic field-effect transistors (OFETs), surface modification of the gate-dielectric is a critical technique for enhancing the electrical properties of the device. Here, we report a simple and versatile method for fabricating an ultrathin cross-linked interlayer (thickness ~3 nm) on an oxide gate dielectric by using polymeric silsesquiazane (SSQZ). The fabricated siloxane film exhibited an ultrasmooth surface with minimal hydroxyl groups; the properties of the surface were chemically tuned by introducing phenyl and phenyl/fluorine pendent groups into the SSQZ. The growth characteristics of two semiconductors—pentacene (p-type) and *N*,*N*′-ditridecyl-3,4,9,10-perylene tetracarboxylic diimide (PTCDI-C13, n-type)—on this ultrathin film were systematically investigated according to the type of pendent groups in the SSQZ-treated gate dielectric. Pentacene films on phenyl/fluorine groups exhibited large grains and excellent crystalline homogeneity. By contrast, PTCDI-C13 films exhibited greater crystalline order and perfectness when deposited on phenyl groups rather than on phenyl/fluorine groups. These microstructural characteristics of the organic semiconductors, as well as the dipole moment of the pendent groups, determined the electrical properties of FETs based on pentacene or PTCDI-C13. Importantly, compared to FETs in which the gate dielectric was treated with a silane-coupling agent (a commonly used surface treatment), the FETs fabricated using the tunable SSQZ treatment showed much higher field-effect mobilities. Finally, surface treatment with an ultrathin SSQZ layer was also utilized to fabricate flexible OFETs on a plastic substrate. This was facilitated by the facile SSQZ deposition process and the compatibility of SSQZ with the plastic substrate.

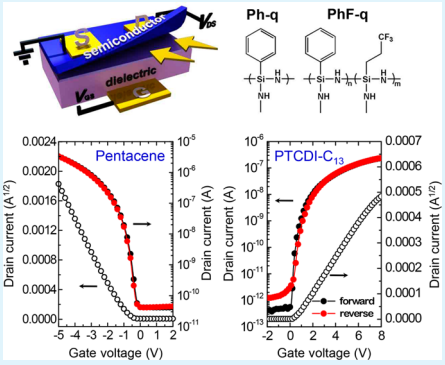

KEYWORDS: *organic field-effect transistors, silsesquiazane, pentacene, N,N′-ditridecyl-3,4,9,10-perylene tetracarboxylic diimide, surface modifier*

1. INTRODUCTION

Much attention has been devoted to developing flexible electronics that can be fabricated on plastic substrates.[1−8] In particular, organic field-effect transistors (OFETs) have emerged as promising devices for use in flexible display backplanes. Although significant effort has been devoted to the realization of flexible OFETs, various issues must still be addressed to enhance their performance. In OFETs, charge carriers pass through the interface between the gate dielectric and semiconductor, making the properties of this interface crucial to device performance.[9,10] Insertion of an ultrathin nanolayer at the interface can significantly change device performance parameters such as the field-effect mobility, current on/off ratio and threshold voltage.[11−14] In this regard, self-assembled monolayers (SAMs) have been widely used to modify the surfaces of common oxide gate-dielectric materials such as SiO_2 or AlO_x in OFETs with a bottom gate structure.[15−20] A typical approach has been to dip the target substrate in a solution containing a silane coupling agent for a couple of hours, resulting in the formation of a nanolayer by reaction-mediated self-assembly. However, SAM formation in such systems is a subtle process involving hydrolysis and condensation. When fabricating the SAM, atmospheric H_2O, solvent type, and reaction temperature must be controlled to obtain a well-organized SAM on which to grow a well-organized organic semiconductor film with low interface trap density.[18,21] If the phase-state and packing density of the SAM are not optimized for subsequent organic semiconductor growth, the electrical properties of the OFET will be degraded significantly.[22]

Received: October 11, 2014
Accepted: December 2, 2014
Published: December 2, 2014

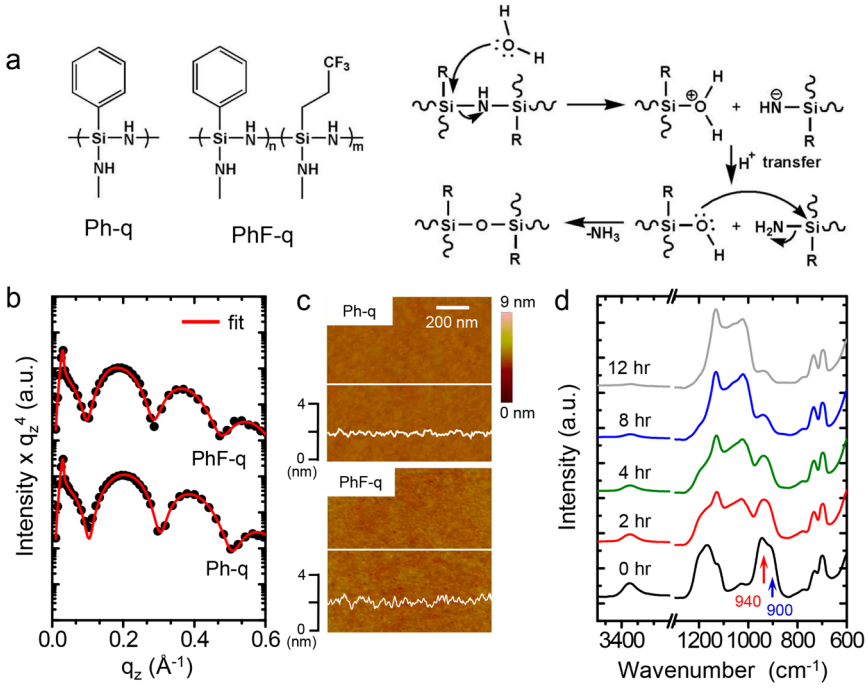

Figure 1. (a, left) Chemical structures of the Ph-SSQZ and PhF-SSQZ used in this study; (right) reaction scheme for Ph-SSQZ and PhF-SSQZ. (b) XRR curves and (c) AFM images of Ph-SSQZ- and PhF-SSQZ-treated SiO_2/Si. (d) FT-IR spectra of the Ph-SSQZ film as a function of annealing time at 150 °C.

As an alternative to the use of a SAM, a spin-coated thin polymer layer (i.e., polystyrene) can be employed to modify the surface characteristics of an inorganic gate-dielectric.[23−25] Because such a polymer layer protects the hydroxyl groups of the oxide gate-dielectric, the charge trap density can be reduced and the electrical properties can be greatly enhanced.[24] However, the polymer layer can be easily destroyed by subsequent processing of the organic semiconductor.[4] In previous works, cross-linked polymers (i.e., polyvinylphenol or poly(vinyl alcohol) with a cross-linking agent) have been used to fabricate a robust polymer film.[11,26,27] However, a drawback of this method is that the residual hydroxyl groups remained in the cross-linked film, which triggered charge trapping and device instability. As a single component cross-linking solution, poly(methyl silsesquioxane) (PMSSQ) was synthesized and a siloxane network film with minimal hydroxyl groups was fabricated by spin coating a PMSSQ solution and subsequent thermal annealing.[28−31] A bulk PMSSQ film or PMSSQ/oxide dual layer was used as a gate-dielectric for high-performance OFETs. However, the surface roughness of the PMSSQ film was relatively high because of the rapid cross-linking reaction. In addition, it was not easy to reduce the thickness of the PMSSQ film down to a few nanometers while maintaining a smooth surface after cross-linking.

In the present study, to overcome the shortcomings of PMSSQ, polymeric silsesquiazane (SSQZ) was spin-coated on an oxide gate-dielectric (SiO_2) to fabricate an ultrathin polymer layer that is chemically anchored on the gate-dielectric. Under humid conditions, Si−OH groups form spontaneously and further annealing at 150 °C leads to a Si−O−Si network with neighboring Si-NH_2 groups or Si−OH groups on SiO_2/Si substrates. Compared to PMSSQ, the SSQZ cross-linking reaction was significantly slower, and thus the cross-linked ultrathin layer (thickness of ∼3 nm) contained a lower density of hydroxyl groups and a smooth surface (roughness of ∼0.4 nm) was uniformly formed on the oxide surface. By introducing phenyl or fluorine pendent groups in SSQZ, it was possible to examine the growth characteristics of representative p-type and n-type organic semiconductors and the variation in the performance characteristics of the resulting OFETs according to the type of pendent groups. Furthermore, flexible p-type and n-type OFETs with a cross-linked SSQZ interlayer were fabricated on plastic substrates.

2. EXPERIMENTAL SECTION

2.1. Materials. SSQZ with phenyl pendant groups (Ph-q) was synthesized by a previously reported method using phenyltrichlorosilane (Aldrich).[32,33] SSQZ with both phenyl and fluorine pendent groups (PhF-q) was synthesized using the following procedure. A 10 wt % solution containing phenyltrichlorosilane and trifluoroethyltrichlorosilane (Aldrich) in pyridine was added to a three-neck flask equipped with a gas inlet and a condenser under a moisture-free nitrogen atmosphere. The solution was cooled to 0 °C with constant stirring, and ammonia gas was introduced. The reaction proceeded for 3 h, after which time excess ammonia was removed by flowing nitrogen through the solution. A white solid salt was removed by filtration under nitrogen. The solvent was removed from the filtrate under vacuum to yield PhF-q. The crude product was redissolved in tetrahydrofuran and purified by reprecipitation from methanol. The resulting white powder was dried under vacuum overnight and stored in a drybox prior to usage. The M_w (8200) and polydispersity index (3.69) of PhF-q were determined using gel permeation chromatography (GPC, Waters), calibrated with narrow MW polystyrene standards.

2.2. Device Fabrication. SSQZ thin films were fabricated by spin-coating a 0.1 wt % solution of SSQZ in tetrahydrofuran (THF) onto a SiO_2 (thickness 300 nm)/Si substrate at 3000 rpm for 60 s, followed by thermal annealing at 150 °C for 12 h. For flexible FETs, AlO_x dielectric (thickness 50 nm) was deposited on an ITO-coated polyethylene naphthalate (PEN) substrate (Tenjin DuPont Films) by a plasma-enhanced atomic layer deposition (PE-ALD) process and the cross-linked SSQZ film was deposited in a manner similar to that used for SSQZ deposition onto the SiO_2/Si substrate. Pentacene or

N,*N*′-ditridecyl-3,4,9,10-perylene tetracarboxylic diimide (PTCDI-C13) was then thermally evaporated onto the SSQZ-treated SiO_2/Si or AlO_x plastic substrates. The Au source/drain electrodes were deposited by thermal evaporation through a metal shadow mask.

2.3. Characterization. The thickness of the SSQZ layer and the crystalline structures of the pentacene and PTCDI-C13 thin-films were investigated using synchrotron X-ray experiments performed at the 5A beamline at the Pohang Accelerator Laboratory (PAL). The chemical structure of the SSQZ layer was confirmed by Fourier transform infrared spectroscopy (FT-IR). The surface morphologies of the SSQZ layer, pentacene, and PTCDI-C13 were characterized by atomic force microscopy (AFM) in tapping mode. The current−voltage characteristics of the FETs were measured using a Keithley 4200-SCS semiconductor parameter analyzer under ambient conditions.

3. RESULTS AND DISCUSSION

Figure 1 shows the mechanism of the cross-linking reaction of SSQZ with phenyl pendent groups (Ph-q) or phenyl/fluorine pendent groups (PhF-q). Via this mechanism, completely cross-linked Si−O−Si networks can be generated by hydrolysis and subsequent condensation reactions of SSQZ.[32,34] Si−N−Si linkages in the SSQZ break into Si−OH and Si−NH_2 groups, and the reactive Si−OH groups attack the Si atom of the Si−NH_2 groups at a mild temperature of 150 °C to form Si−O−Si bonds with release of NH_3. During the process, the condensation reaction can also be preceded with the Si−OH groups in the SiO_2/Si substrate and it is possible to fabricate a robust ultrathin layer on the SiO_2/Si substrate. X-ray reflectivity (XRR) profiles of fabricated SSQZ films with Ph-q and PhF-q on SiO_2/Si substrates showed that the films were ultrathin layers with thicknesses of around ∼3 nm (Figure 1b and Table 1). In addition, atomic force microscopy (AFM) images showed smooth surface morphologies (roughness ∼0.4 nm) (Figure 1c). These findings demonstrate that the cross-linked SSQZ film is uniform and ultrathin, characteristics that are required for efficient surface modification of inorganic gate-dielectrics such as SiO_2 or Al_2O_3. To examine the chemical structure of the SSQZ layer as a function of annealing time at 150 °C, FT-IR spectra were measured of films annealed for up to 12 h (Figure 1d). The peaks at 940 and 3365 cm^{-1}, which correspond to Si−N and N−H stretching vibrations, respectively,[32,33] dramatically decreased as the annealing time was increased. This can be explained by hydrolysis in the Si-NH-Si linkage. On the other hand, the peak at 1025 cm^{-1}, which was not discernible prior to annealing, increased sharply with increasing annealing time. This vibrational peak derives from the Si−O−Si linkage. From these results, the proposed reaction mechanism as shown in Figure 1a can be rationalized. Because the signal at 900 cm^{-1} associated with Si−OH groups becomes negligible after 12 h of annealing at 150 °C, the characteristics of the remaining OH groups can be elucidated.[30,31] The chemical stability of the Ph-q or PhF-q was tested by immersing the SSQZ-treated SiO_2/Si substrate into common organic solvents such as chloroform and toluene. We observed no change in the thickness or surface morphology of the film, confirming the chemical inertness of the Ph-q and PhF-q. As expected from the low surface energy of fluorine groups, the surface energy of PhF-q was much lower than that of Ph-q (Table 1). In summary, a Ph-q or PhF-q layer can be uniformly deposited onto a SiO_2/Si substrate via a mechanism involving hydrolysis and a polycondensation reaction, and the resulting ultrathin and robust layer provides a smooth surface ready for efficient gate-dielectric functioning in OFETs.

Table 1. Surface Characteristics of Untreated and Ph-SAM-, Ph-SSQZ-, and PhF-SSQZ-Treated SiO_2 Dielectrics

dielectric surface modification	dielectric surface properties		
	thickness (nm)	surface roughness (nm)	surface energy (mJ/m^2)
bare			
Ph-SAM	0.8 (±0.2)	0.3 (±0.1)	42.8 (±3.1)
Ph-SSQZ	3.1 (±0.2)	0.4 (±0.1)	41.4 (±2.8)
PhF-SSQZ	3.3 (±0.1)	0.4 (±0.2)	31.9 (±1.7)

To examine the effects of SSQZ treatment on the growth characteristics of p-type/n-type organic semiconductors, we thermally evaporated pentacene (p-type) or PTCDI-C13 (n-type) on top of SSQZ-treated SiO_2/Si substrates. Figure 2a shows AFM images of pentacene films (thickness 50 nm) deposited on three substrate types: untreated and Ph-SSQZ- and PhF-SSQZ-treated SiO_2 dielectrics. The pentacene grains on the Ph-q substrate had much smaller grain sizes than those on the PhF-q substrate. This can be attributed to the lower surface energy of PhF-q giving rise to a lower nucleation density. The grain size of pentacene on PhF-q is comparable to or even higher than that on bare (untreated) SiO_2. Because the Ph-q and PhF-q surfaces are smooth, the growth behavior on the ultrathin layers is not affected by heterogeneous nucleation. Figure 3b shows AFM images of 50 nm thick PTCDI-C13 films on the three types of substrate. All of the films showed similar rod-like morphologies of crystalline PTCDI-C13 molecules. However, although the morphology of the organic semiconductor films are similar, the molecular ordering and crystalline microstructure within the films may differ.

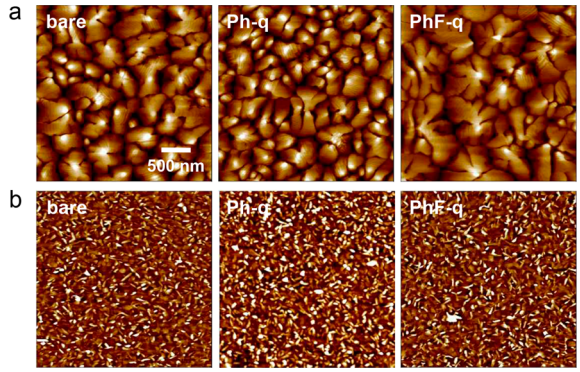

Figure 2. AFM images of 50 nm thick (a) pentacene and (b) PTCDI-C13 films deposited on untreated and Ph-SSQZ- and PhF-SSQZ-treated SiO_2 dielectrics.

Figure 3 shows the structural characteristics of pentacene films on the three substrate surfaces. Normal mode XRD scans of untreated (bare) SiO_2 (Figure 3a) exhibited (00*l*) diffractions of the thin-film crystalline phase (a = 5.946 Å, b = 7.558 Å, γ = 89.77°, $d_{(001)}$ = 15.5 Å), with small peaks corresponding to the bulk crystalline phase (indicated by arrows in the higher order peaks).[35] These two polymorphs are typical in thermally evaporated pentacene thin-film where thin-film crystalline phase is energetically less stable than bulk crystalline phase. For the two types of SSQZ-treated SiO_2 substrate, however, only peaks corresponding to the thin-film crystalline phase were detected, although their intensities were smaller than those of pentacene on the untreated SiO_2. This result indicates that surface treatment of the SiO_2 with a

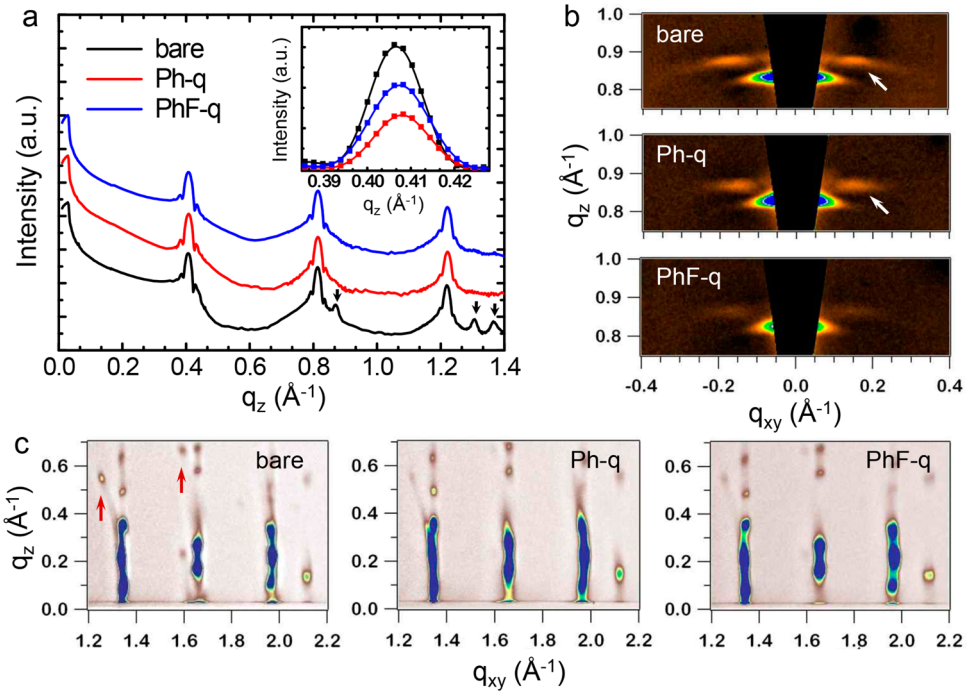

Figure 3. (a) XRD patterns of 50 nm thick pentacene films deposited on untreated and Ph-SSQZ- and PhF-SSQZ-treated SiO_2 dielectrics; (inset) enlarged (001) peak of the XRD pattern. The 2D GIXD patterns along the (b) q_z and (c) q_{xy} directions, corresponding to the out-of-plane and in-plane directions of the pentacene films, respectively.

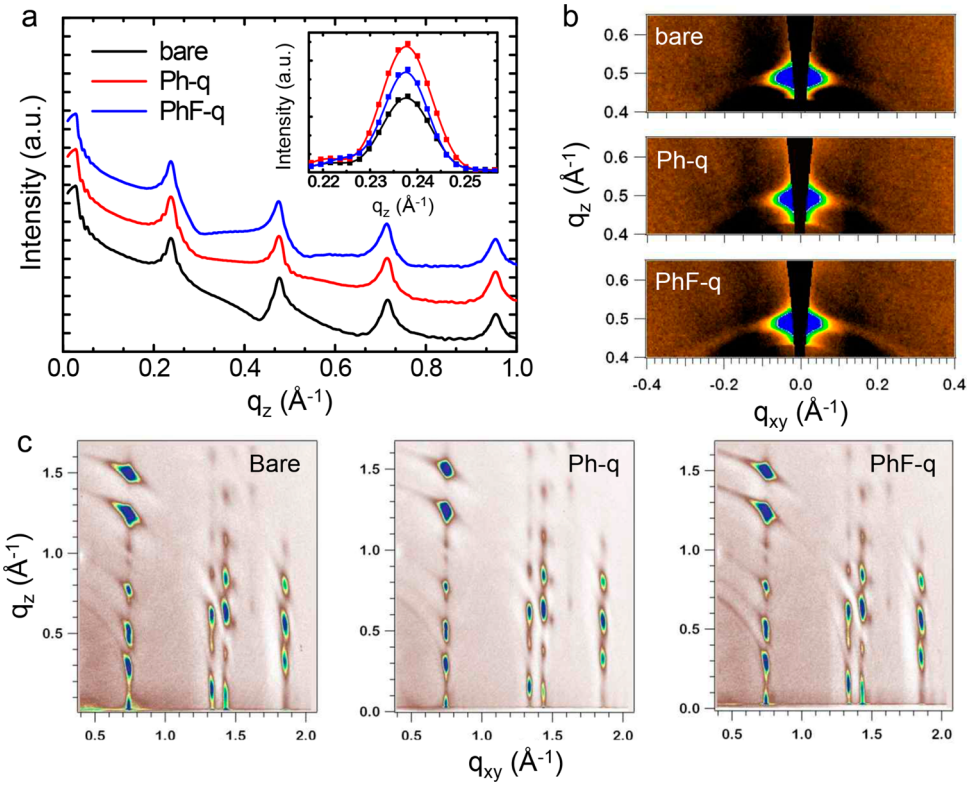

Figure 4. (a) XRD patterns of the 50 nm thick PTCDI-C13 films deposited onto untreated and Ph-SSQZ- and PhF-SSQZ-treated SiO_2 dielectrics; (inset) enlargement of the (001) peak of the XRD pattern. The 2D GIXD patterns along the (b) q_z and (c) q_{xy} directions, corresponding to the out-of-plane and in-plane directions of the PTCDI-C13 film, respectively.

hydrophobic SSQZ layer increases the crystalline homogeneity of the pentacene film. Interestingly, when PhF-q was used, the (00*l*) peak intensity increased considerably compared to the system with Ph-q (Figure 3a, inset). Grazing incidence X-ray diffraction (GI-XD) showed a pronounced difference in the pentacene crystalline structure depending on the surface characteristics of the substrate. Figure 3b shows diffuse scattering intensities of (002) diffraction peaks along the

Debye rings. Because diffuse scattering originated from the crystal mismatch of pentacene, the small diffuse scattering observed in PhF-q is indicative of crystal homogeneity of pentacene from this surface. Remarkably, (002) diffraction peaks corresponding to bulk crystalline phase is slightly tilted with respect to the surface normal direction (q_z, indicated by white arrow in bare and Ph-q). On the other hand, such tilted crystalline phases are barely detected for pentacene on the PhF-q substrate. In accordance with the out-of-plane reflection pattern, three intense in-plane reflections, {1, ±1}, {0, 2}, {1, ±2} in the thin film phase reflections,[36] appear nearly vertically at a given q_{xy} for the system with a PhF-q substrate (Figure 3c). On the other hand, the observation of tilted in-plane reflections for the untreated SiO_2 (indicated by red arrows) matches well with the tilted bulk crystalline phase along the out-of-plane direction (Figure 3b). This finding confirms that, in this system, the bulk crystalline phase, which is slightly tilted along q_z direction, significantly contributes to the overall crystalline structure of pentacene. Thus, the crystalline homogeneity of pentacene decreases in the following order: PhF-q > Ph-q > bare (untreated) SiO_2.

PTCDI-C13 exhibits preferential molecular ordering due to its long alkyl chains. When PTCDI-C13 grows on a substrate surface, it forms (00*l*) planes oriented parallel to the surface in order to minimize the surface energy.[37−40] Accordingly, normal mode XRD patterns of PTCDI-C13 films deposited onto untreated and Ph-SSQZ- and PhF-SSQZ-treated SiO_2 dielectrics (Figure 4a) only show (00*l*) diffraction spots. The intensity of the (002) diffraction (Figure 4a, inset) decreases in the following order: Ph-q > PhF-q > bare (untreated) SiO_2. Because the edge-on orientation with alkyl chains exposed to the substrate surface is beneficial for the π-overlap of conjugated planes, preferential orientation with (00*l*) planes oriented normal to the surface can contribute to the lateral transport of charge carriers.[37] Figure 4b shows the angular spread of (00*l*) diffraction spots. The PTCDI-C13 film on Ph-q exhibited lower angular spread than that on PhF-q. The GI-XD patterns in Figure 4c show Bragg rod in-plane reflections along the q_z direction at a given q_{xy}, which can be indexed as {0,1}, {1,0}, {1, ±1}, {1, ±2}.[13] These in-plane reflections originate from the π-overlap of conjugated planes and their azimuthal spreads are directly correlated with the distortion of the crystal planes. The XRD pattern of the PTCDI-C13 film on Ph-q exhibits the lowest tilting of the in-plane reflections, indicating that this film has the lowest degree of lattice distortion. On PhF-q, by contrast, the lateral growth of molecules is prohibited a little. Further study is underway to investigate the reasons for this behavior. It should be emphasized that SSQZ with only ∼3 nm thickness can affect growth characteristics of organic semiconductors (i.e., pentacene, PTCDI-C13) differently by having different functional groups.

To investigate the correlation between growth characteristics of organic semiconductors and the electrical properties of OFETs, we deposited Au source/drain electrodes directly onto pentacene or PTCDI-C13 films. Figure 5 shows the output and transfer curves of pentacene FETs and PTCDI-C13 FETs. For comparison, devices were also fabricated using phenyltrichlorosilane to modify the SiO_2/Si substrate surface; the phenyl-terminated SAM (Ph-SAM) was fabricated by immersing a SiO_2/Si substrate in phenyltrichlorosilane solution in toluene for 1 h. The pentacene FET with PhF-q exhibited a higher on-current than did the corresponding device using Ph-q (Figure 5a). The electrical properties were further examined by

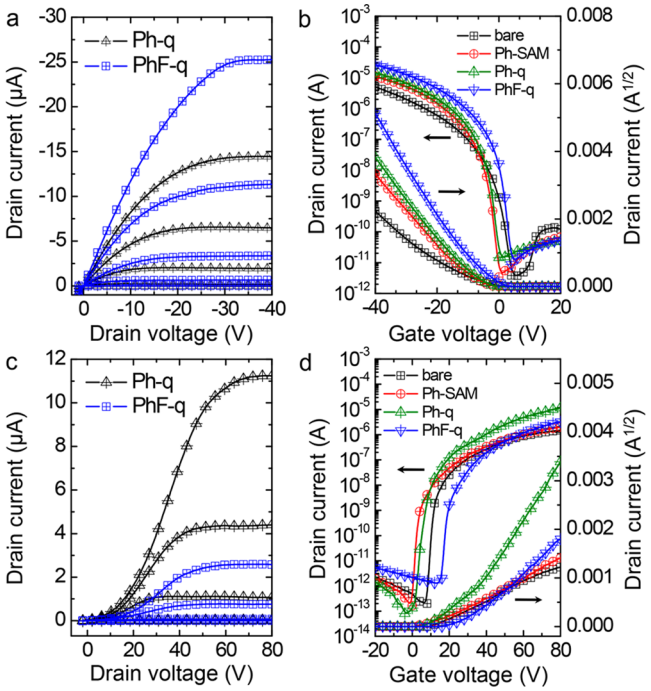

Figure 5. (a) Output characteristics of pentacene FETs with gate dielectrics modified by Ph-SSQZ or PhF-SSQZ. (b) Transfer characteristics of pentacene FETs with untreated and Ph-SAM-, Ph-SSQZ-, and PhF-SSQZ-treated SiO_2 dielectrics where drain voltage is fixed at −40 V. (c) Output characteristics of PTCDI-C13 FETs with gate dielectrics modified by Ph-SSQZ or PhF-SSQZ. (d) Transfer characteristics of PTCDI-C13 FETs with untreated and Ph-SAM-, Ph-SSQZ-, and PhF-SSQZ-treated SiO_2 dielectrics where drain voltage is fixed at 80 V.

analyzing the transfer characteristics (Figure 5b); the results are summarized in Table 2. The field-effect mobilities of pentacene FETs calculated from the saturation regime in the transfer characteristics decreased in the following order: PhF-q > Ph-q > Ph-SAM > bare. The mobility of 0.60 (±0.14) $cm^2/(V\ s)$ obtained using PhF-q could be further increased by changing the operating conditions of the evaporator or by using a pentacene source with high purity. The high mobility in the PhF-q device can be attributed to the combined effect of the large grain size (Figure 2a) and crystalline homogeneity (Figure 3). By contrast, the PTCDI-C13 FETs exhibited a different trend in the field-effect mobility: Ph-q > PhF-q > Ph-SAM > bare. The higher mobility in the Ph-q device can be explained by the structural analysis in Figure 4, which showed that PTCDI-C13 on Ph-q had higher crystalline order and perfectness compared to that on PhF-q. Interestingly, all the FET devices suffer from large charge injection barriers, as indicated by nonlinear behavior at the low drain voltage of the output characteristics (Figure 5c). This is caused by the use of Au source/drain electrodes with high work function that exhibit large mismatch with LUMO level of PTCDI-C13. For this reason, all the electrical properties of PTCDI-C13 FET devices shown in Table 2 were extracted from the transfer characteristics at the saturation regime (drain voltage of 80 V). Thus, we surmise that the effects of charge injection in four different types of the dielectric surface (i.e., bare, Ph-SAM, Ph-q, PhF-q) are nearly the same, and comparative explanation is still valid. Although Ph-q and Ph-SAM contain the same phenyl group, the electrical properties of organic semiconductor layers

dx.doi.org/10.1021/am507003n | ACS Appl. Mater. Interfaces 2014, 6, 22807−22814

Table 2. Electrical Properties of OFET Devices Based on Pentacene or PTCDI-C13 as the Semiconductor and SiO_2 Dielectrics Whose Surfaces Were Untreated or Treated with Ph-SAM, Ph-SSQZ, or PhF-SSQZ

	pentacene			PTCDI-C13		
dielectric surface modification	field-effect mobility ($cm^2/(V\ s)$)	ON/OFF current ratio	V_{th} (V)	field-effect mobility ($cm^2/(V\ s)$)	ON/OFF current ratio	V_{th} (V)
bare	0.12 (±0.08)	1.3×10^6	−12.5 (±3.7)	0.007 (±0.003)	7.5×10^6	11.1 (±4.9)
Ph-SAM	0.25 (±0.07)	3.3×10^6	−8.3 (±2.5)	0.012 (±0.005)	1.2×10^7	12.5 (±4.6)
Ph-SSQZ	0.41 (±0.11)	1.0×10^6	−8.9 (±2.8)	0.11 (±0.03)	8.7×10^7	23.5 (±5.1)
PhF-SSQZ	0.60 (±0.14)	3.0×10^6	−6.8 (±1.5)	0.03 (±0.01)	2.6×10^6	29.2 (±7.2)

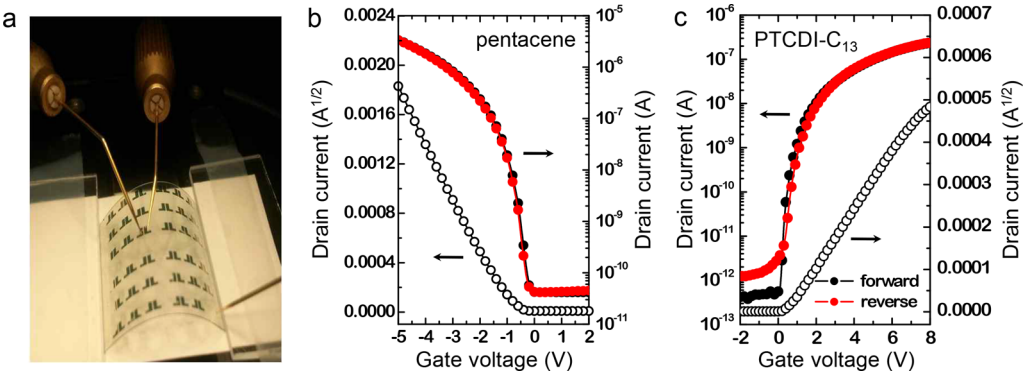

Figure 6. (a) Photograph of flexible, transparent pentacene FETs on a Ph-SSQZ-treated AlO_x/ITO/PEN substrate. (b) Transfer characteristics of pentacene FETs (measured at the drain voltage of −5 V) and (c) PTCDI-C13 FETs (measured at the drain voltage of 8 V) on plastic substrates.

deposited on substrates modified with Ph-q and Ph-SAM were quite different. The surface coverage of Ph-SAM might not be high due to the short alkyl chain of Ph-SAM. Thus, it is not as effective as Ph-q or PhF-q for constructing a full-coverage surface modification layer without hydroxyl groups. For this reason, the field-effect mobilities of pentacene or PTCDI-C13 FETs with Ph-SAMs are much lower than those with Ph-q. Interestingly, for both pentacene and PTCDI-C13 FETs, the threshold voltage (V_{th}) and turn-on voltage (V_{on}) shifted depending on the functional group in SSQZ. FETs with PhF-q showed positively shifted V_{th} and V_{on} compared to FETs with Ph-q. This behavior can be attributed to the dipole moment of the fluorine groups that accumulate hole carriers (p-type) or deplete electron carriers (n-type).[41−43] This result demonstrates that SSQZ treatment can be used to control V_{th} and V_{on} by adopting different functional groups in SSQZ.

To investigate the potential application of SSQZ treatment for the fabrication of flexible transistors, p-type/n-type organic transistors were constructed on a PEN substrate. To impart low-voltage operation to the flexible transistors, a thin aluminum oxide (AlO_x) dielectric layer of thickness 50 nm (specific capacitance = 140 nF/cm^2) was deposited on an indium tin oxide (ITO)-coated PEN substrate by plasma-enhanced atomic layer deposition (PE-ALD). Subsequently, an ultrathin Ph-q layer was deposited on the AlO_x/ITO/PEN substrate by spin-coating, and then a semiconductor layer and source/drain electrodes were deposited in a similar manner to that used for the SiO_2/Si substrate. The SSQZ molecules react with the hydroxyl groups in AlO_x followed by a polycondensation process, which leads to the formation of an ultrathin SSQZ layer on the AlO_x/ITO/PEN substrate. Figure 6a shows a photographic image of the flexible/transparent pentacene FETs on a plastic substrate, and Figure 6b shows their electrical properties. It should be noted that the transfer characteristics of the FETs do not display hysteresis under dual sweeps when the devices are operated at low voltage (below −5 V). Because Ph-q provides an ultrathin cross-linked layer with minimal unreacted silanol or amino groups, charge trapping between the organic semiconductor and dielectric is minimized. Thus, the pentacene FETs on a flexible substrate showed a high mobility of 0.3 ± 0.04 $cm^2/(V\ s)$ with negligible hysteresis. The extremely low hysteresis is due to the unique properties of Ph-q without hydroxyl groups. Although the PTCDI-C13 FETs on a flexible substrate also exhibited negligible hysteresis (Figure 6c), the field-effect mobility was only 0.02 ± 0.01 $cm^2/(V\ s)$. We speculate that the low mobility in the flexible PTCDI-C13 FETs might originate from the rough plastic substrate. It is inferred from our experiment that the effect of roughness on the electrical performances of OFETs can be different depending on the molecular structure and microstructure of organic semiconductors. Postdeposition annealing can be used to further enhance the electrical properties of PTCDI-C13 FETs.[37,38]

4. CONCLUSIONS

We have utilized ultrathin cross-linked SSQZ layers with different functional groups to modify the surface properties of the gate-dielectric in n-type/p-type OFETs. The growth characteristics of pentacene or PTCDI-C13 molecules on the SSQZ layers were mainly determined by the functional groups in the SSQZ (i.e., Ph-q or PhF-q). Pentacene films deposited on PhF-q had large grains and excellent crystalline homogeneity. As a result, pentacene FETs with PhF-q exhibited excellent electrical properties. By contrast, PTCDI-C13 showed higher crystalline order and perfectness when deposited on Ph-q rather than PhF-q. In accordance with these microstructural characteristics, PTCDI-C13 FETs with Ph-q exhibited a much higher field-effect mobility than the corresponding devices with PhF-q or Ph-SAM. Surface treatment with an ultrathin SSQZ layer was also efficient for fabricating flexible OFETs on a flexible plastic substrate because of the facile deposition process and compatibility with the plastic substrate. The present

findings indicate that ultrathin cross-linked SSQZ layers without residual hydroxyl groups are a promising alternative to commonly used SAMs for enhancing the electrical properties of OFETs and enabling flexible electronics.

AUTHOR INFORMATION

Corresponding Author

*E-mail: jhcho94@skku.edu.

Author Contributions

[∇]W. H. Lee and S. G. Lee contributed equally to this work.

Notes

The authors declare no competing financial interest.

ACKNOWLEDGMENTS

This research was supported by Basic Science Research Program through the NRF of Korea funded by the Ministry of Education, Science and Technology (2012R1A2A2A04047240 and 2009-0083540), and the World-Class 300 Project (development of organic materials with high transmittance, high insulating properties, and high flexibility for next-generation display) funded by the Small and Medium Business Administration of Korea (SMBA).

REFERENCES

(1) Forrest, S. R. The Path to Ubiquitous and Low-Cost Organic Electronic Appliances on Plastic. *Nature* **2004**, *428*, 911−918.

(2) Cho, J. H.; Lee, J.; Xia, Y.; Kim, B.; He, Y. Y.; Renn, M. J.; Lodge, T. P.; Frisbie, C. D. Printable Ion-Gel Gate Dielectrics for Low-Voltage Polymer Thin-Film Transistors on Plastic. *Nat. Mater.* **2008**, *7*, 900−906.

(3) Katz, H. E. Recent Advances in Semiconductor Performance and Printing Processes for Organic Transistor-based Electronics. *Chem. Mater.* **2004**, *16*, 4748−4756.

(4) Kang, B.; Lee, W. H.; Cho, K. Recent Advances in Organic Transistor Printing Processes. *ACS Appl. Mater. Interfaces* **2013**, *5*, 2302−2315.

(5) Moonen, P. F.; Yakimets, I.; Huskens, J. Fabrication of Transistors on Flexible Substrates: from Mass-Printing to High-Resolution Alternative Lithography Strategies. *Adv. Mater.* **2012**, *24*, 5526−5541.

(6) Zhao, Y.; Di, C. A.; Gao, X. K.; Hu, Y. B.; Guo, Y. L.; Zhang, L.; Liu, Y. Q.; Wang, J. Z.; Hu, W. P.; Zhu, D. B. All-Solution-Processed, High-Performance n-Channel Organic Transistors and Circuits: Toward Low-Cost Ambient Electronics. *Adv. Mater.* **2011**, *23*, 2448−2453.

(7) Yi, H. T.; Payne, M. M.; Anthony, J. E.; Podzorov, V. Ultra-Flexible Solution-Processed Organic Field-Effect Transistors. *Nat. Commun.* **2012**, *3*, 1259.

(8) Kaltenbrunner, M.; Sekitani, T.; Reeder, J.; Yokota, T.; Kuribara, K.; Tokuhara, T.; Drack, M.; Schwodiauer, R.; Graz, I.; Bauer-Gogonea, S.; Bauer, S.; Someya, T. An Ultra-Lightweight Design for Imperceptible Plastic Electronics. *Nature* **2013**, *499*, 458−463.

(9) Miozzo, L.; Yassar, A.; Horowitz, G. Surface Engineering for High-Performance Organic Electronic Devices: the Chemical Approach. *J. Mater. Chem.* **2010**, *20*, 2513−2538.

(10) Park, Y. D.; Lim, J. A.; Lee, H. S.; Cho, K. Interface Engineering in Organic Transistors. *Mater. Today* **2007**, *10*, 46−54.

(11) Yoon, M. H.; Yan, H.; Facchetti, A.; Marks, T. J. Low-Voltage Organic Field-Effect Transistors and Inverters Enabled by Ultrathin Cross-Linked Polymers as Gate Dielectrics. *J. Am. Chem. Soc.* **2005**, *127*, 10388−10395.

(12) Park, S. H.; Lee, H. S.; Kim, J. D.; Breiby, D. W.; Kim, E.; Park, Y. D.; Ryu, D. Y.; Lee, D. R.; Cho, J. H. A Polymer Brush Organic Interlayer Improves the Overlying Pentacene Nanostructure and Organic Field-Effect Transistor Performance. *J. Mater. Chem.* **2011**, *21*, 15580−15586.

(13) Kim, S. H.; Jang, M.; Yang, H.; Anthony, J. E.; Park, C. E. Physicochemically Stable Polymer-Coupled Oxide Dielectrics for Multipurpose Organic Electronic Applications. *Adv. Funct. Mater.* **2011**, *21*, 2198−2207.

(14) Park, K.; Park, S. H.; Kim, E.; Kim, J. D.; An, S. Y.; Lim, H. S.; Lee, H. H.; Kim, D. H.; Ryu, D. Y.; Lee, D. R.; Cho, J. H. Polymer Brush As a Facile Dielectric Surface Treatment for High-Performance, Stable, Soluble Acene-Based Transistors. *Chem. Mater.* **2010**, *22*, 5377−5382.

(15) Liao, K. C.; Ismail, A. G.; Kreplak, L.; Schwartz, J.; Hill, I. G. Designed Organophosphonate Self-Assembled Monolayers Enhance Device Performance of Pentacene-Based Organic Thin-Film Transistors. *Adv. Mater.* **2010**, *22*, 3081−3085.

(16) Klauk, H.; Zschieschang, U.; Pflaum, J.; Halik, M. Ultralow-Power Organic Complementary Circuits. *Nature* **2007**, *445*, 745−748.

(17) DiBenedetto, S. A.; Facchetti, A.; Ratner, M. A.; Marks, T. J. Molecular Self-Assembled Monolayers and Multilayers for Organic and Unconventional Inorganic Thin-Film Transistor Applications. *Adv. Mater.* **2009**, *21*, 1407−1433.

(18) Ito, Y.; Virkar, A. A.; Mannsfeld, S.; Oh, J. H.; Toney, M.; Locklin, J.; Bao, Z. A. Crystalline Ultrasmooth Self-Assembled Monolayers of Alkylsilanes for Organic Field-Effect Transistors. *J. Am. Chem. Soc.* **2009**, *131*, 9396−9404.

(19) Nakayama, K.; Uno, M.; Nishikawa, T.; Nakazawa, Y.; Takeya, J. Air-Stable and High-Mobility Organic Thin-Film Transistors of Poly(2,5-bis(2-thienyl)-3,6-dihexadecyltheino[3,2-b]thiophene) on Low-Surface-Energy Self-Assembled Monolayers. *Org. Electron.* **2010**, *11*, 1620−1623.

(20) Acton, O.; Dubey, M.; Weidner, T.; O'Malley, K. M.; Kim, T. W.; Ting, G. G.; Hutchins, D.; Baio, J. E.; Lovejoy, T. C.; Gage, A. H.; Castner, D. G.; Ma, H.; Jen, A. K. Y. Simultaneous Modification of Bottom-Contact Electrode and Dielectric Surfaces for Organic Thin-Film Transistors Through Single-Component Spin-Cast Monolayers. *Adv. Funct. Mater.* **2011**, *21*, 1476−1488.

(21) Lee, H. S.; Kim, D. H.; Cho, J. H.; Hwang, M.; Jang, Y.; Cho, K. Effect of the Phase States of Self-assembled Monolayers on Pentacene Growth and Thin-Film Transistor Characteristics. *J. Am. Chem. Soc.* **2008**, *130*, 10556−10564.

(22) Virkar, A.; Mannsfeld, S.; Oh, J. H.; Toney, M. F.; Tan, Y. H.; Liu, G. Y.; Scott, J. C.; Miller, R.; Bao, Z. The Role of OTS Density on Pentacene and C-60 Nucleation, Thin Film Growth, and Transistor Performance. *Adv. Funct. Mater.* **2009**, *19*, 1962−1970.

(23) Sun, X. N.; Zhang, L.; Di, C. A.; Wen, Y. G.; Guo, Y. L.; Zhao, Y.; Yu, G.; Liu, Y. Q. Morphology Optimization for the Fabrication of High Mobility Thin-Film Transistors. *Adv. Mater.* **2011**, *23*, 3128−3133.

(24) Yoon, M. H.; Kim, C.; Facchetti, A.; Marks, T. J. Gate Dielectric Chemical Structure-Organic Field-Effect Transistor Performance Correlations for Electron, Hole, and Ambipolar Organic Semiconductors. *J. Am. Chem. Soc.* **2006**, *128*, 12851−12869.

(25) Wang, Y.; Acton, O.; Ting, G.; Weidner, T.; Shamberge, P. J.; Ma, H.; Ohuchi, F. S.; Castner, D. G.; Jen, A. K. Y. Effect of the Phenyl Ring Orientation in the Polystyrene Buffer Layer on the Performance of Pentacene Thin-Film Transistors. *Org. Electron.* **2010**, *11*, 1066−1073.

(26) Jang, Y.; Kim, D. H.; Park, Y. D.; Cho, J. H.; Hwang, M.; Cho, K. W. Low-Voltage and High-Field-Effect Mobility Organic Transistors with a Polymer Insulator. *Appl. Phys. Lett.* **2006**, *88*, 072101−072103.

(27) Veres, J.; Ogier, S. D.; Leeming, S. W.; Cupertino, D. C.; Khaffaf, S. M. Low-k Insulators as the Choice of Dielectrics in Organic Field-Effect Transistors. *Adv. Funct. Mater.* **2003**, *13*, 199−204.

(28) Wu, Y. L.; Liu, P.; Ong, B. S. Organic Thin-Film Transistors with Poly(methyl silsesquioxane) Modified Dielectric Interfaces. *Appl. Phys. Lett.* **2006**, *89*, 013505−013507.

(29) Bao, Z. N.; Kuck, V.; Rogers, J. A.; Paczkowski, M. A. Silsesquioxane Resins as High-Performance Solution Processible Dielectric Materials for Organic Transistor Applications. *Adv. Funct. Mater.* **2002**, *12*, 526−531.

(30) Jeong, S.; Kim, D.; Lee, S.; Park, B. K.; Moon, J. Organic–Inorganic Hybrid Dielectrics with Low Leakage Current for Organic Thin-Film Transistors. *Appl. Phys. Lett.* **2006**, *89*, 092101–092103.
(31) Nagase, T.; Hamada, T.; Tomatsu, K.; Yamazaki, S.; Kobayashi, T.; Murakami, S.; Matsukawa, K.; Naito, H. Low-Temperature Processable Organic–Inorganic Hybrid Gate Dielectrics for Solution-Based Organic Field-Effect Transistors. *Adv. Mater.* **2010**, *22*, 4706–4710.
(32) Yoo, K. H.; Kim, I. W.; Cho, J. H.; Kwark, Y. J. Silsesquiazane/Organic Polymer Blends as Organic–Inorganic Hybrid Materials. *Fibers Polym.* **2012**, *13*, 1113–1119.
(33) Lee, H. S.; Park, K.; Kim, J. D.; Han, T.; Ryu, K. H.; Lim, H. S.; Lee, D. R.; Kwark, Y. J.; Cho, J. H. Interpenetrating Polymer Network Dielectrics for High-Performance Organic Field-Effect Transistors. *J. Mater. Chem.* **2011**, *21*, 6968–6974.
(34) Kozuka, H.; Nakajima, K.; Uchiyama, H. Superior Properties of Silica Thin Films Prepared from Perhydropolysilazane Solutions at Room Temperature in Comparison with Conventional Alkoxide-Derived Silica Gel Films. *ACS Appl. Mater. Interfaces* **2013**, *5*, 8329–8336.
(35) Lee, J. S.; Kim, N. H.; Kang, M. S.; Yu, H.; Lee, D. R.; Oh, J. H.; Chang, S. T.; Cho, J. H. Wafer-Scale Patterning of Reduced Graphene Oxide Electrodes by Transfer-and-Reverse Stamping for High Performance OFETs. *Small* **2013**, *9*, 2817–2825.
(36) Kim, D. H.; Lee, H. S.; Yang, H. C.; Yang, L.; Cho, K. Tunable Crystal Nanostructures of Pentacene Thin Films on Gate Dielectrics Possessing Surface-Order Control. *Adv. Funct. Mater.* **2008**, *18*, 1363–1370.
(37) Jang, J.; Nam, S.; Chung, D. S.; Kim, S. H.; Yun, W. M.; Park, C. E. High T_g Cyclic Olefin Copolymer Gate Dielectrics for *N*,*N*′-Ditridecyl Perylene Diimide Based Field-Effect Transistors: Improving Performance and Stability with Thermal Treatment. *Adv. Funct. Mater.* **2010**, *20*, 2611–2618.
(38) Tatemichi, S.; Ichikawa, M.; Koyama, T.; Taniguchi, Y. High Mobility n-type Thin-Film Transistors based on *N*,*N*′-ditridecyl Perylene Diimide with Thermal Treatments. *Appl. Phys. Lett.* **2006**, *89*, 112108–112110.
(39) Hong, K.; Kim, S. H.; Yang, C.; Jang, J.; Cha, H.; Park, C. E. Improved n-Type Bottom-Contact Organic Transistors by Introducing a Poly(3,4-ethylenedioxythiophene):poly(4-styrene sulfonate) Coating on the Source/Drain Electrodes. *Appl. Phys. Lett.* **2010**, *97*, 103304–103306.
(40) Chesterfield, R. J.; McKeen, J. C.; Newman, C. R.; Ewbank, P. C.; da Silva, D. A.; Bredas, J. L.; Miller, L. L.; Mann, K. R.; Frisbie, C. D. Organic Thin Film Transistors based on N-alkyl Perylene Diimides: Charge Transport Kinetics as a Function of Gate Voltage and Temperature. *J. Phys. Chem. B* **2004**, *108*, 19281–19292.
(41) Jang, Y.; Cho, J. H.; Kim, D. H.; Park, Y. D.; Hwang, M.; Cho, K. Effects of the Permanent Dipoles of Self-Assembled Monolayer-Treated Insulator Surfaces on the Field-Effect Mobility of a Pentacene Thin-Film Transistor. *Appl. Phys. Lett.* **2007**, *90*, 132104–132106.
(42) Kobayashi, S.; Nishikawa, T.; Takenobu, T.; Mori, S.; Shimoda, T.; Mitani, T.; Shimotani, H.; Yoshimoto, N.; Ogawa, S.; Iwasa, Y. Control of Carrier Density by Self-Assembled Monolayers in Organic Field-Effect Transistors. *Nat. Mater.* **2004**, *3*, 317–322.
(43) Pernstich, K. P.; Haas, S.; Oberhoff, D.; Goldmann, C.; Gundlach, D. J.; Batlogg, B.; Rashid, A. N.; Schitter, G. Threshold Voltage Shift in Organic Field Effect Transistors by Dipole Monolayers on the Gate Insulator. *J. Appl. Phys.* **2004**, *96*, 6431–6438.